Irradiation Behavior of Uranium-Molybdenum Dispersion Fuel: Fuel Performance Data from RERTR-1 and RERTR–2

M.K. Meyer, G.L. Hofman*, J.L. Snelgrove*, C.R. Clark, S.L. Hayes, and R.V. Strain*
Argonne National Laboratory
P.O. Box 2528, Idaho Falls ID 83403 and *1700 S. Cass Avenue, Argonne, IL 60439, USA

J.M. Park, K.H. Kim
Korea Atomic Energy Research Institute
150, Dukjin-Dong, Yusong-Ku, Taejon, 305-353, Korea

ABSTRACT

This paper presents quantitative data on the irradiation behavior of uranium-molybdenum fuels from the low temperature RERTR-1 and -2 experiments. Fuel swelling measurements of U-Mo fuels at ~40% and ~70% burnup are presented. The rate of fuel-matrix interaction layer growth is estimated. Microstructures of fuel in the pre- and post-irradiation condition were compared. Based on these data, a qualitative picture of the evolution of the U-Mo fuel microstructure during irradiation has been developed. Estimates of uranium-molybdenum fuel swelling and fuel-matrix interaction under high-power research reactor operating conditions are presented.

INTRODUCTION

Over the past two years, the RERTR-1 and –2 experiments have been fabricated, irradiated, and examined. The purpose of these experiments was to obtain initial irradiation performance data on a variety of uranium alloy dispersion fuels, allowing more refined subsequent irradiation tests to be performed on those alloys that show promise.

RERTR-1 was discharged from the ATR after 94 effective full-power days (EFPDs) of irradiation at calculated peak burnups between 39 and 45 at.% ^{235}U. RERTR-2 was discharged following 232 EFPDs at calculated burnups between 65 and 71 at.% ^{235}U. The fuel centerline temperature of these plates during irradiation was calculated to be approximately 65°C. A series of U-Mo and U-Nb-Zr fuels were irradiated to differentiate compositional effects. Atomized U-10Mo and U-10Mo filings were included in the test matrix in order to differentiate between fuels of the same composition but different microstructure. Post-irradiation examination has concentrated on analysis of the better performing uranium-molybdenum alloy series containing 6% to 10% by weight of alloying elements from the high burnup RERTR-2 test vehicle. Fission density and burnup for the fuels discussed here are given in Table 1. Performance of other fuels are discussed elsewhere in these proceedings. [1]

Table 1. Fission density and burnup of irradiated fuel test coupons

Plate ID	Fuel composition (wt%)	^{235}U burnup* (peak %)	Core fission density (10^{21} cm^{-3})	Fuel fission density (10^{21} cm^{-3})	Avg. fuel fission rate (10^{14} cm^{-3} s^{-1})
A005	U-10Mo	69	1.4	4.9	2.4
V003	U-10Mo	70	0.9	5.0	2.5
B004	U-8Mo	70	1.4	5.2	2.6
M003	U-6Mo-0.6Ru	68	1.5	5.2	2.6
C003	U-6Mo	67	1.4	5.2	2.6

*calculated

EXPERIMENTAL METHODS

The fuel test coupons exhibited little dimensional growth during irradiation, and dimensional measurements were not useful in establishing a ranking for fuel swelling among the U-Mo alloy fuels. Fuel swelling measurements were thus made by quantitative metallography through selection and measurement of objects on the basis of image contrast. Quantitative metallography provides an indirect measurement of swelling, since measurements are made on a plane area, rather than on a volume. The assumption is made that the two dimensional measurements are from a random cross section with no preferred orientation, so that area fraction is representative of volume fraction. To cross-check and validate results of fuel area measurements, measurements of fission gas bubble area and fuel aluminum interaction layer thickness were made.

Fuel area measurements were made from montages of micrographs taken on as-polished longitudinal cross sections of fuel plates. Manual correction was made to the images to exclude non-fuel foreign matter, such as tungsten carbide particles present as a by-product of powder production. There was very little porosity or fuel pullout that required interpretation. Since the fuel distribution in the plates may not be strictly uniform, some error is introduced by choosing a random section that is assumed to be representative of the entire fuel plate. This uncertainty was estimated by measuring the fuel area at random locations along the length of fuel plates and is estimated to be ±2% of the measurement. Since all plates containing fuel filings were loaded to the same volume fraction and fabricated using the same procedure, an overall average initial fuel area fraction of 33 % was assigned to these plates. The measured as-fabricated area fraction of the U-10Mo atomized fuel is 28.3 %.

Bubble area measurements were made using a combination of SEM and optical images. After polishing, SEM samples were etched for 3-5 minutes in an aqueous solution of 10% nitric acid and 10% hydrogen peroxide. Magnification of SEM images was 7,500X to 10,000X, allowing resolution of bubbles as small as 0.1 μm. The area fraction of bubbles in the diameter range 0.1- 1 μm was measured using SEM images. The area of bubbles larger than 1 μm in diameter was determined using 500X optical images of as-polished specimens. Some manual correction to both image types was required, as contrast variations due to sample topography were sometimes interpreted as pores.

Measurements of the thickness of the fuel-aluminum interaction layer as a function of burnup were taken from both SEM and optical micrographs. SEM fracture specimens were prepared by punching out a 1.6 mm diameter disc through the fuel zone and fracturing the punching through the fuel zone and parallel to the cladding. Flat regions of the fracture surface were compared to optical and SEM images of polished sections to obtain a reaction layer thickness. Since such measurements are skewed to larger values by oblique sectioning angles, a 'common minimum' value was established.

Calculation of fuel particle swelling values based on these measurements compounds the relatively large uncertainty inherent in these measurements. For this reason differential fuel area swelling values reported here must be considered approximate, with an error of ±8%.

FUEL SWELLING MEASUREMENTS

The primary contributions to fuel swelling are reaction of the fuel with the aluminum matrix, solid fission product formation, and fission gas bubble nucleation and growth. The sum of the swelling due to each of these mechanisms should approximate the total fuel swelling, since the processes are largely independent in these fuel specimens. It was estimated that solid fission products account for 0.2% volume swelling per percent ^{235}U burnup. [2]

Measured post-irradiation fuel area fractions, fission gas bubble areas, and interaction layer thickness are given in Table 2. The values for fuel area fraction given in Table 2 are relative to the area of the fuel meat and include the area of the entire fuel particle, including the area produced due to interaction with the matrix. Fission gas bubble area is relative to the area of the irradiated fuel particle.

Table 2. Fuel area fraction, gas bubble area, and interaction layer thickness

	Measured Fuel Area Fraction		Fission Gas Bubble Area	Interaction Layer Thickness (μm)	
Fuel Composition	~ 40% burnup	~ 70% burnup	~ 70% burnup	~ 40% burnup	~ 70% burnup
U-10Mo atomized	0.293	0.39	0.057	1.7	2.6
U-10Mo filings	0.345	0.48	0.095	1.7	2.6
U-8Mo	*	0.52	*	2.0	2.8
U-6Mo-0.6Ru	*	0.58	*	2.0	3.5
U-6Mo	*	0.61	0.12	*	3.7

*Not measured

Representative micrographs of polished, etched, and fractured fuel particle cross sections for the high burnup U-10Mo and U-6Mo fuels are shown in Figure 1. The U-6Mo fuel exhibits a bimodal bubble distribution, with approximately 4% of the bubble area present as bubbles of size larger than 1 μm visible in 500X optical micrographs. The remainder of the bubble area is present as smaller bubbles of size 0.1-1 μm visible in SEM images.

The fission gas bubble area trends with the observed fuel swelling behavior in that U-6Mo > U-10Mo filings > U-10Mo atomized. The U-10Mo atomized fuel contains regions where no visible bubbles are present (Figure 1(a), center), contributing to the decreased fission gas bubble area.

Direct measurement of the fuel/aluminum interaction area on the irregular fuel filings was difficult for two reasons. Most importantly, the measured interaction area will be an overestimate of the true area due to the oblique sectioning angles of the irregular fuel particles on the observed metallographic cross section. Secondly, contrast variations on optical micrographs of suitably large areas were lost in the noise produced by sample preparation defects. Large areas of high-contrast SEM images were not available due to operational limitations. As an alternative to direct measurement of interaction area, the perimeter to area ratio of the fuel in the as-fabricated state was measured from a metallographic cross-section. This ratio was found to be 0.122 μm^{-1}. An equivalent circular area of 33 μm diameter was then assigned as the fuel particle size for the fuel filings. Calculations based on measured interaction layer thickness and assigned diameter were then used to estimate area increase due to interaction layer growth. An iterative calculation was performed to determine the amount of swelling due to aluminide formation and the recession of the original interface due to consumption of the alloy to form the aluminide. It was assumed from thermal diffusion data that the interaction layer was $(U,Mo)Al_3$, where the U/Mo ratio in the intermetallic was the same as that in the alloy. A decrease in $(U,Mo)Al_3$ reaction product density from 6.8 g/cm^3 concomitant with the decrease in alloy density as a function of molybdenum content was assumed.

As a check on the validity of the method used to estimate fuel swelling due to fuel-aluminum interaction, interaction area measurements were made on U-6Mo and U-8Mo metallographic cross-sections from plates C003 and B004. Interaction areas were manually highlighted due to difficulties in obtaining images suitable for direct analysis. The resulting measured area fractions are 29.1% for U-8Mo and 35.3% for U-6Mo. These compare well to the calculated interaction areas of 28% for U-8Mo and 35% for U-6Mo based on the model described above.

The actual particle size distribution was measured for a U-10Mo atomized fuel plate using the Johnson-Saltykov diameter method to normalize data from an as-fabricated fuel plate section [3]. The area weighted mean diameter was found to be 68 μm.

In the case of U-6Mo, there was significant fuel growth due to reaction during fabrication. The amount of this growth was estimated by comparison of actual as-fabricated fuel area to the as-fabricated area of U-10Mo plates. The U-10Mo plates did not undergo significant reaction during fabrication. The U-6Mo fuel had a pre-irradiation fuel area fraction of 0.385, translating into a fuel area swelling of 17% during fabrication (0.33 vs. 0.385) and a calculated reaction area of 18% of the fuel area. This calculation was cross-checked by measuring the reacted area on a U-6Mo as-fabricated metallographic section from an SEM/BSE image. Reaction area and was found to be 14% of the total fuel area. This translates to 12% fuel swelling in reasonable agreement with the swelling value of 17% calculated by the difference in U-10Mo and U-6Mo as-fabricated fuel areas.

DISCUSSION

Illustrations of the relative contributions to measured fuel area at ~ 70% burnup from growth of fission gas bubbles, fuel/matrix interaction, and solid fission product formation are shown in Figure 2 in comparison to measured swelling. Note that the data for U-10Mo atomized powder are corrected to a fuel loading of 33%. In all cases, the measured post-irradiation fuel area is within 3% of the area of the sum of the measured and estimated swelling components (Figure 2), lending credibility to the methods and measurements. Area swelling values are tabulated in Table 3.

Table 3. Contributions to fuel swelling

Fuel	Approx. contribution to fuel particle $\Delta A/A^d$ (%)				Total fuel particle $\Delta A/A^d$ (%) (measured)	Estimated fuel meat swelling ($\Delta V/V$ %)
	$(U,Mo)Al_3$ (irradiation)	UAl_x (fabrication)	fission gas	sfp[b]		
U-10Mo	24	1	14	9	48 (45)	10±4
U-10Mo[a]	14	0	8	9	31 (38)	8±4
U-8Mo	26	2	18[c]	9	55 (58)	11±4
U-6Mo	35	12	22	9	78 (85)	12±5

a-atomized powder
b-solid fission products
c-estimated from interpolation of U-10Mo and U-6Mo data
d-uncertainty ±8% of reported value

Fuel matrix interaction

Figure 2 shows that formation of an aluminide interaction layer is the most significant contribution to swelling in these fuels under low temperature, high-burnup irradiation conditions. This condition exists due to the high uranium density of the fuel and the stoichiometry of the reaction. It is more severe than in lower density compounds such as U_3Si_2.

Measured interaction layer thickness for U-xMo fuels irradiated in RERTR-1 and –2 is plotted in Figure 3 as a function of fission density. Also plotted in Figure 3 is data for U_3Si and U_3Si_2 fuel irradiated in ORR at approximately 100°C, and data for U_3Si_2 irradiated in RERTR-1 and -2. The growth of the interaction layer on silicide fuels [4] as a function of temperature and fission density follows the correlation given as formula (1).

(1) $Y = [K^{irr}F^{n}(t\text{-}to)\exp\{-Q^{irr}/RT\}]^{1/2} + [K^{th}(t\text{-}to)\exp\{-Q^{th}/RT\}]^{1/2}$

Where Y is the interaction layer thickness, superscript *irr* indicates growth due to in-reactor athermal processes, superscript *th* indicates thermally activated processes, T is the dispersion temperature, n=1, Q^{irr}=5.42 kcal/mole, $K^{irr}=5.07\times10^{-26}$, $K^{th}=9.3\times10^{12}$, and Q^{th}=83.4 kcal/mole. At the temperatures and fission rates considered here, contributions due to the thermal component play no role.

Interaction layer growth behavior of U-10Mo and U-8Mo fuels appears to be well described by the silicide correlation, as shown by the fit of the data to the lower line. Correlation of U-6Mo and U-6Mo-X fuels require some adjustment, however too few data are available to determine a modified correlation.

As an example of the effects of fuel-aluminum interaction during irradiation, aluminum depletion of the matrix was modeled for 8.0 gU/cm^3 U-8Mo spheres to a fuel burnup of 90% ^{235}U. The temperature at which 10 volume percent of the fuel matrix remains as un-reacted aluminum after irradiation is shown as a function of particle size in Figure 4. It can be seen that small particles (fines) are consumed and will deplete the matrix of aluminum during irradiation, even near room temperature. In contrast, larger fuel particles do not deplete the matrix of aluminum until substantially higher temperatures. The net result is that aluminum depletion does not appear to be a significant problem for fuels at this loading if attention is given to fuel particle size. Interaction layer thickness, fuel particle volume increase, and fuel meat swelling (due to interaction) are shown in Figure 5 as a function of fission density for the case a 150 μm sphere at 175°C and the same loading and fuel density as above. At 60% burnup, a 7 μm thick interaction layer is predicted and fuel particle volume swelling will be 22.0%, but total fuel meat swelling due to reaction is only 1%.

Aluminum depletion was found, under certain irradiation conditions, to result in excessive void formation in U_3Si_2 dispersion fuel samples. This deleterious effect appears to follow the rapid formation of the phase $U(Si,Al)_3$ when matrix aluminum is not present. The depletion of aluminum in itself does not necessarily result in void formation. For example, UAl_2-Al dispersions have been irradiated with virtually complete aluminum depletion to high burnup without any evidence of void formation. [5] A drastic change in diffusion kinetics, such as may occur through the formation of a new phase, seems to be required to affect excessive void formation.

Inspection of the U-Mo-Al ternary system does not indicate that such a situation exists here, however this system is not as well characterized as the U-Si-Al system. Several RERTR-3 test specimens are designed to provide the needed information on this question.

Microstructural effects

The inclusion of two U-10Mo fuels with different microstructures allows some conclusions to be drawn about the effects of microstructure on fuel swelling. Fuel particle swelling for U-10Mo atomized fuel was measured as 38±3% (Table 3). For U-10Mo filings, the swelling was measured at 45±4%. The primary difference in the measurements is the swelling due to interaction of the fuel with the matrix. In the case of U-10Mo ground powder this accounted for 24±2% of the total swelling, whereas it accounts for only 14±1% in the atomized powder. This is due to the larger area weighted mean diameter of the atomized powder of 68 μm versus 33 μm (effective) for the U-10Mo filings. There are also clear differences in the mechanism for nucleation and growth of fission gas bubbles, as shown in Figure 1 and verified by gas bubble area measurements. The atomized fuel shows areas with no visible fission gas bubbles.

Based on measurements of gas bubble area, fission gas driven swelling accounts for 14±1% of fuel area increase in the filings and 8±1% in the atomized powder. It has been shown that the atomized fuel powder has segregated areas of high and low molybdenum content. [6] The pattern of the bubble formation in the irradiated fuel mirrors the pattern of segregation in the as-fabricated fuel. [1] Consistent with observations here, molybdenum rich areas in the atomized fuel may be less prone to fission gas bubble nucleation and growth than molybdenum depleted areas. Another possible explanation for the difference is that fission gas bubbles in metallic fuel require defects such as sub-grain boundaries to nucleate. Fuel powder filings will have high dislocation densities due to the large amount of cold deformation introduced during powder production. The times and temperatures during fabrication combined with the effects of irradiation may be sufficient to allow these dislocations to form sub-grains, which might act as nucleation sites for fission gas bubbles. [7] Recrystallization in atomized fuel, however, must be driven solely by irradiation induced damage and recovery and may have a longer onset time.

Compositional effects

Fuel swelling is found to decrease with increasing alloy content for the series of U-xMo fuels. Again, a primary effect is due to formation of the fuel/matrix interaction layer. In the case of U-6Mo, significant fuel particle growth occurred during fabrication (Table 3). This, combined with significant reaction during irradiation, resulted in a $\Delta A/A$ that was significantly higher than in the other fuels. Fission gas driven swelling, as approximated by gas bubble area, also has a discernable compositional dependence. Comparison of U-10Mo filings with U-6Mo filings shows that U-10Mo has a lower fission gas bubble area; optical micrographs of polished sections in Figure 1 shows that a higher density of large gas bubbles has been generated in U-6Mo during irradiation. Based on measurements of gas bubble area, fission gas driven swelling accounts for 22±2% of fuel area increase in U-6Mo and 14±1% in U-10Mo.

It appears that the addition of the gamma stabilizer ruthenium did not produce an effect on swelling (Table 2) beyond what would be expected from the addition of an equivalent amount of molybdenum. X-ray diffraction indicates that the fuel in the U-6Mo fuel plate has undergone considerable decomposition from the gamma phase during fuel plate fabrication. However, it has also been shown that at irradiation temperatures of less than 200°C, equilibrium $\alpha + \gamma'$ (U_2Mo) structures with sufficient alloy content to be quenchable to the metastable γ phase will revert to γ on irradiation to burnup on the order of 0.1%. [8,9]

Estimation of Fuel Meat Volume Swelling

In order to estimate fuel meat volume swelling, the fuel meat area changes due to estimated fuel-matrix interaction, fission gas bubble growth, and solid fission product formation were summed and converted to volume change. This methodology takes into account the consumption of matrix aluminum that is not apparent from fuel particle swelling measurements. In order to translate area change into volume change, some description of particle shape must be assumed; a sphere was used here for simplicity.

The change in volume of a sphere in terms of the area change of a circular section through the center is given by equation (2).

(2) $\Delta V/V = (\Delta A/A+1)^{3/2} - 1$

Volume swelling estimates are given in Table 3 for the fuels considered here. These are rough estimates, since unknown uncertainties are introduced in the arbitrary choice of particle shape, and differential swelling errors are further compounded. The total volume change for the U-10Mo, U-8Mo, and U-6Mo fuel meats irradiated in RERTR-2 is on the order of 4-16%. It is for this reason that dimensional measurement of the small RERTR-1 and -2 test coupons was not effective in differentiating the swelling behavior of the fuels.

CONCLUSION

Analysis of U-Mo fuels from the RERTR-1 and –2 tests have shown that in general, fuels with six weight percent or more molybdenum content perform well during irradiation at low temperatures. Fuel particle swelling decreases as alloy content increases from six to ten weight percent. The largest contribution to fuel swelling is from the growth of the fuel/aluminum interaction layer. This swelling is a function of fuel composition and accounts for much of the compositional difference in swelling behavior. The interaction layer growth correlation developed for silicide fuels provides a good description of the data for interaction layer growth in U-8Mo and U-10Mo. This model predicts that matrix aluminum depletion occurs rapidly above 100°C due to the large amount of uranium available in the fuel. This effect is a strong function of surface area to volume ratio and could be offset by increasing fuel particle size.

Fission gas driven swelling, as approximated by gas bubble area, is affected to some degree by both composition and microstructure. Comparison of U-10Mo atomized particles with U-10Mo filings indicates that the atomized fuel powder shows less gas bubble nucleation and growth. Comparison of U-10Mo filings with U-6Mo filings shows that U-10Mo has less fission gas driven swelling. The primary difference is due to growth of a distribution of larger bubbles in U-6Mo.

The RERTR-3 test currently under irradiation has been designed to provide more information about high temperature interaction behavior, the behavior of the interaction phase, the effects of microstructure, and the effects of gamma stabilizers on irradiation performance.

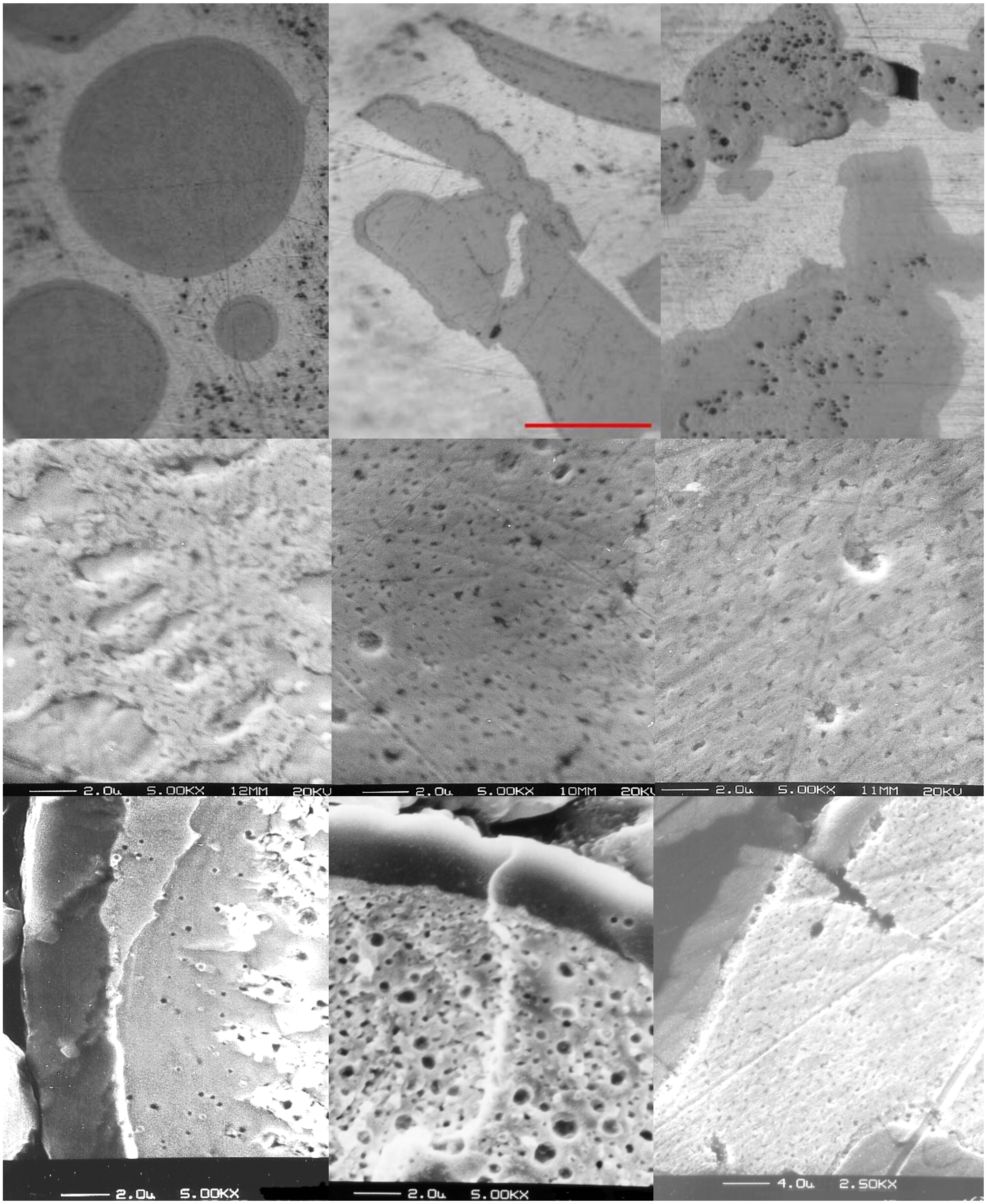

Figure 1. Left to right: (a) U-10Mo atomized fuel, (b) U-10Mo fuel filings, (c) U-6Mo filings. Top, optical image showing large scale porosity. Scale bar = 50 µm. Center, SEM images of etched specimens showing fine-scale porosity. Bottom, SEM images of fracture surfaces showing interaction layer. Note scale difference in U-6Mo image (c).

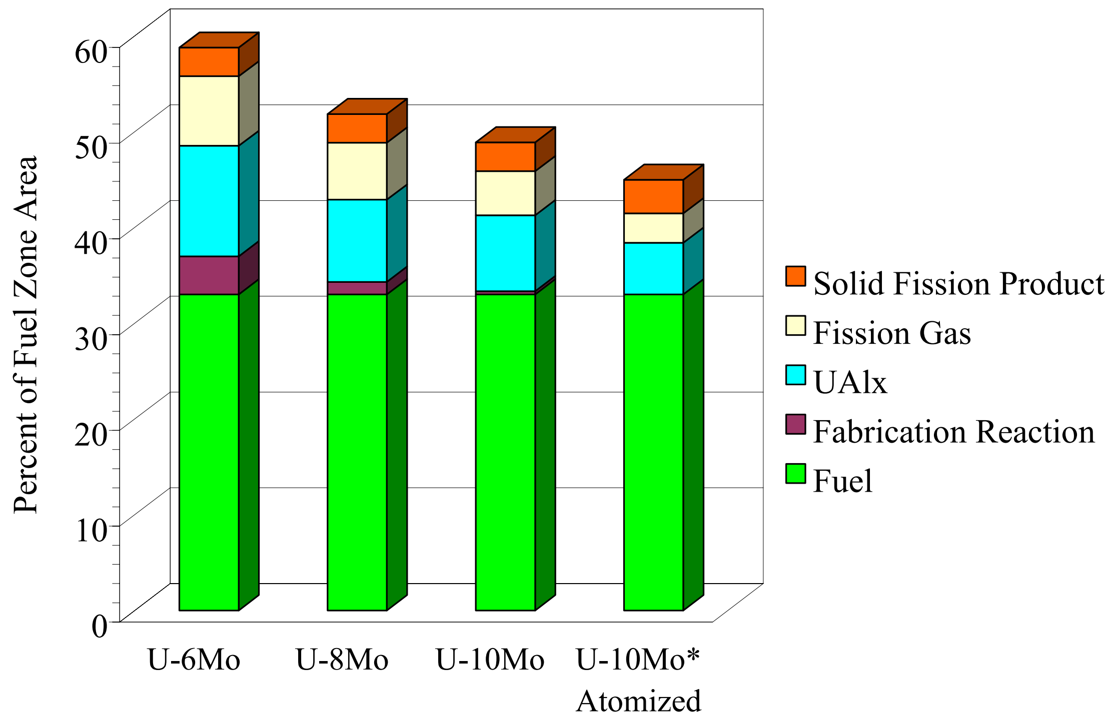

Figure 2. Contributions to fuel area swelling due to fuel-matrix interaction during irradiation (estimate), fuel-matrix interaction during fabrication (measured), fission gas (measured), and solid fission products (estimate). Solid line is measured fuel particle area fraction. Note that U-10Mo atomized data is normalized to 33% initial volume loading.

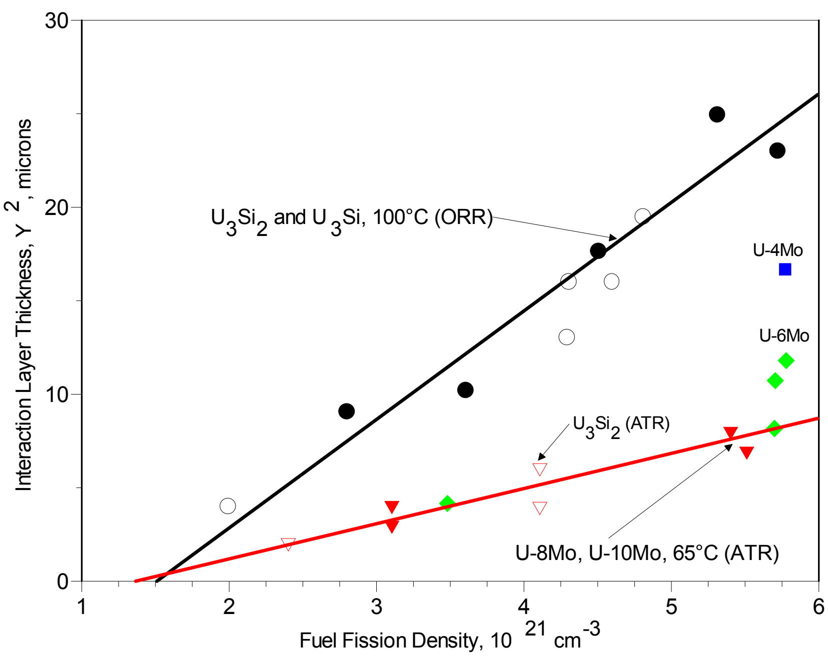

Figure 3. Fuel matrix interaction layer growth for U-Mo and silicide fuels from ATR (Advanced Test Reactor) and ORR (Oak Ridge Reactor) experiments.

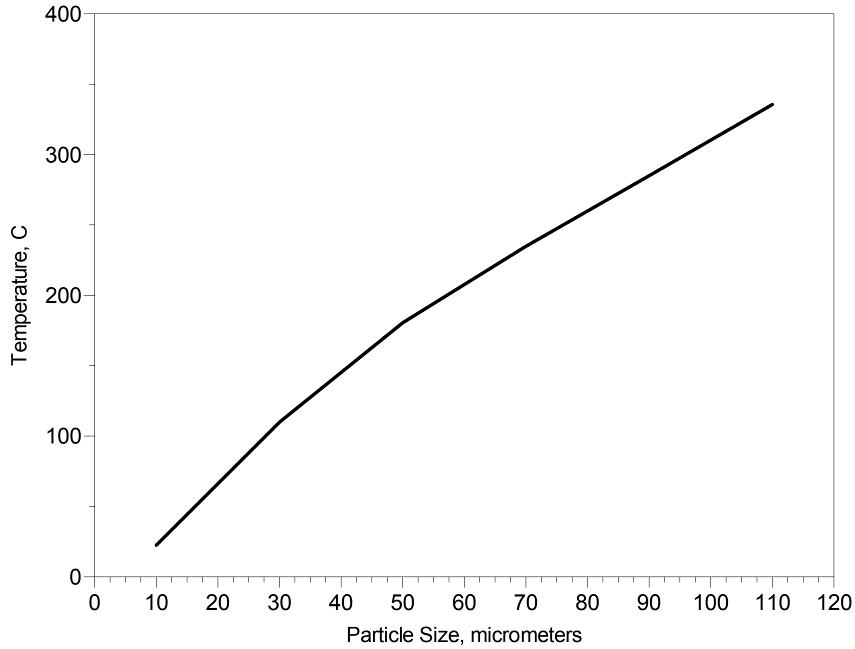

Figure 4. Temperature at which 10 $^{v}/_{o}$ aluminum remains in 8 gU/cm^3 U-8Mo fuel meat after 90% ^{235}U burnup (LEU). Shown as a function of fuel particle size.

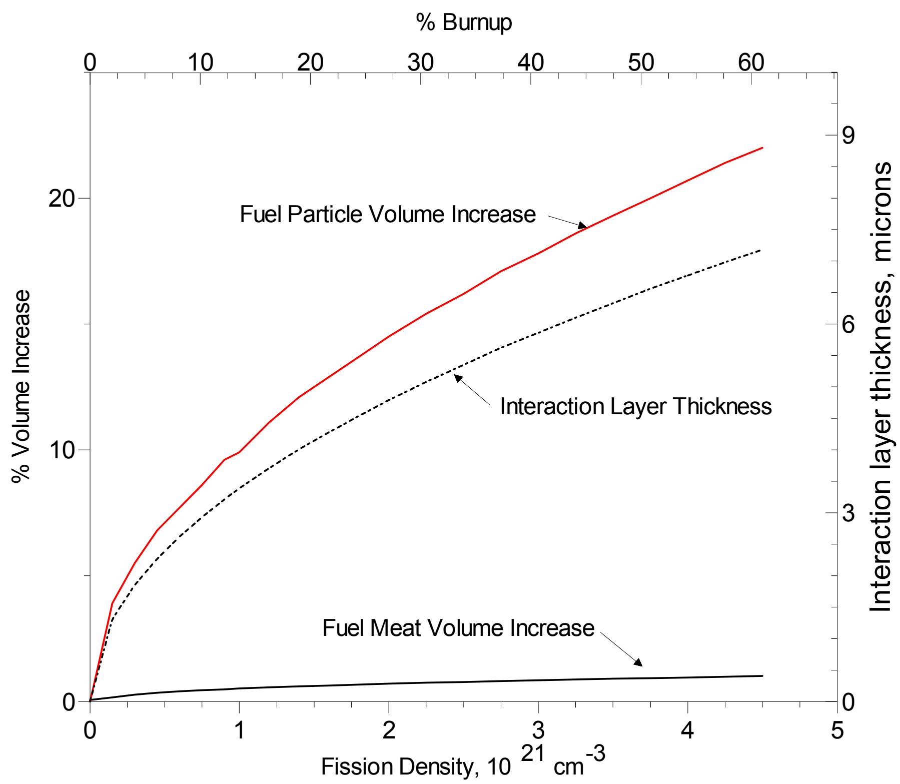

Figure 5. Fuel particle swelling, interaction layer thickness, and fuel meat swelling due to fuel aluminum interaction in 150 μm diameter U-8Mo at 8 gU/cm^3 and 175°C.

REFERENCES

[1] G.L. Hofman, M.K. Meyer, R.V. Strain, "Review of Postirradiation Results of High-Density Fuel Experiments RERTR-1 and RERTR-2," *these proceedings.*

[2] G.L. Hofman, L.C. Walters, T.H. Bauer, "Metallic Fast Reactor Fuels," *Progress in Nuclear Energy* **31** [1/2] 83-110 (1997).

[3] R.T. DeHoff, F.N. Rhines, *Quantitative Microscopy*, McGraw Hill (1968).

[4] G.L. Hofman, J. Rest, J.L. Snelgrove, T.C. Weincek, S. Koster van Groos, "Aluminum-U3Si2 Interdiffusion and its Implications for the Performance of Highly Loaded Fuel Operating at Higher Temperatures and Fission Rates," *Proc. of the 1996 International Meeting on Reduced Enrichment for Research and Test Reactors*, Seoul, South Korea, October 7-10 (1996).

[5] J. Gómez, R. Morando, E.E. Pérez, D.R. Giorsetri, G.L. Copeland, G.L. Hofman, J.L. Snelgrove, "Postirradiation Examination of High-U-Loaded, Low-Enriched U_3O_8, UAl_2, and U_3Si Test Fuel Plates," *Proc. of the 1984 International Meeting on Reduced Enrichment for Research and Test Reactors*, Argonne, IL, Oct 15-18 (1984).

[6] K.-H. Kim, J.M. Park, C.K. Kim, G.L. Hofman, "Stable In-reactor Performance of U-10wt%Mo Dispersion Fuel Prepared with Centrifugally Atomized Powder," *these proceedings.*

[7] J. Rest, G.L. Hofman, I. Konovalov, A. Maslov, "Experimental and Calculated Swelling Behavior of U-10Mo Under Low Irradiation Temperatures," *Proc. of the 1998 International Meeting on Reduced Enrichment for Research and Test Reactors*, Sao Paulo, Brazil (1998).

[8] M.L. Bleiberg, L.J. Jones, B. Lustman, "Phase Changes in Pile Irradiated Uranium Alloys," *J. App. Phys.* **27** [11] 1270-83 (1956).

[9] M.L. Bleiberg, "Effect of Fission Rate and Lamella Spacing upon the Irradiation-Induced Phase Transformation of U-9 wt% Mo Alloy," *J. Nuc. Mat.* **2** 182-90 (1959).